DROPLET SIZE DISTRIBUTION MEASUREMENTS OF ISO NOZZLES BY SHADOWGRAPHY METHOD

N. DE COCK[1], M. MASSINON[1], S. OULED TALEB SALAH[1,2], B. C. N. MERCATORIS[1] AND F. LEBEAU[1]

[1] Liege University, Gembloux Agro-Bio Tech, Biosystems Engineering Department
[2] Liege University, Gembloux Agro-Bio Tech, AgricultureIsLife Platform
Corresponding author E-mail: Nicolas.DeCock@doct.ulg.ac.be

SUMMARY

The droplet size distribution of agricultural sprays is a key parameter during the plant protection product applications. Therefore, measurement of the drop size distribution is an important concern for spray users as well as nozzle manufacturers. The present work assessed the capability of a shadowgraphy technique to distinguish correctly the 6 spray class boundaries defined in the ISO draft standard (ISO 25358).
The measurement set-up is composed by a high speed camera synchronized with a LED backlighting. The tested spray is positioned between the camera and the light. The droplets appear on the images as shadows on a brighter background. For each acquisition, two frames are recorded within a small time laps (38 µs). The droplet diameter and velocity are retrieved by using advanced image analysis algorithm on each pair of frames. Then, the drop size distribution is obtained by gathering the data retrieved from all the images.
The global results showed that the 6 drop size distributions were correctly separated highlighting the ability of the method to measure small as well as large droplets using the same set-up configuration. The spatial analysis showed that the spray scanning should be extended in the minor axis direction in order to catch the whole spray.

Key words: Droplet size distribution, agricultural spray, image analysis, pesticide application, flat fan nozzles

INTRODUCTION

Nowadays, the use of plant protection products is still required to satisfy the growing demand for agricultural goods. During this process the agricultural mixture is atomized by passing through a nozzle generating a cloud of droplets. It has been proved that droplet size distribution has a significant effect on the global deposition process efficiency (Matthews, 2008). Therefore, consequent efforts have been done to classify sprays with respect to their droplet size distributions leading to the creation of 7 spray classes: Very Fine (VF), Fine (F), Medium (M), Coarse (C), Very Coarse (VC), Extremely Coarse (XC) and Ultra Coarse (UC). The boundaries of these classes are defined by 6 sprays produced by 6 different nozzles under a specific pressure which are defined in the ISO draft standard (ISO 25358).
The rapid development of imaging equipments and image processing capabilities during the last decade makes shadowgraphy an ever easier and cheaper alternative to scattering or diffraction based measurement methods for low density spray as agricultural sprays. A number of manufacturers propose off-the shelf systems using proprietary software. A digital PIV-camera combined with standard optics and pulsed Light Emitting Diodes (LED) arrays as light source provide a relatively low cost acquisition system. This equipment can also be used for qualitative observations such as liquid sheet break-up (Cousin et al., 2012) or agricultural spray impact retention (Massinon and Lebeau, 2012)(Massinon et al., 2014), that results in a very versatile tool for laboratories involved in spray application

processes. The previous paper presents a gathering of the recent technical developments in shadow image processing in order to develop an accurate, versatile and low-cost tool to characterize agricultural nozzle spray quality (De Cock et al., 2014). The present work aims to assess the capability of the method to distinguish the 6 spray quality boundaries defined by the ISO draft standard (ISO 25358) for the classification of droplet size spectra from atomizers.

MATERIALS AND METHODS

Image acquisitions set-up

Shadowgraphy involves a backlighted arrangement for image acquisition (Figure 1). A PIV camera (X-Stream™ XS-3, IDT) coupled with high magnification optics provides a field of view of 10x12 mm at a working distance of 130 mm. The spatial resolution is equal to 9.7 µm/pixel. With this magnification factor, droplets with a diameter ranging from 40 to 3500µm can be measured. The minimum droplet size is defined as 4 pixels of diameter and the maximum droplet size is restricted by the field of view size. The lighting is ensured by a custom made 72 W LED array (24 Luxeon III Star White LEDs) placed at 500 mm far from the camera. A LED-controller (PP600F, Gardasoft Vision) provides a control of the LED lighting. The controller is synchronized using the camera external trigger. Digital images are 1024 × 1280 with pixel values ranging from 0 to 255 according to the local light intensity. Droplets appear on images as darker regions on a brighter background. In order to avoid motion blur a short exposure time is used (~3µs). Using the double exposure mode of the PIV camera, two consecutive images are acquired within a short time (38 µs) allowing the computation of the droplet displacements and then in turn the droplet velocities.
The technique probe volume corresponds to the volume in which the droplets appear sharp enough to be measured with an acceptable error (<5%). A droplet has to appear in both frame of a pair image to be taking in account therefore the size of the probe volume is decreasing with the droplet speed. Calibrations showed that this volume is a rectangular parallelepiped with a maximum size of 10x12x1mm.

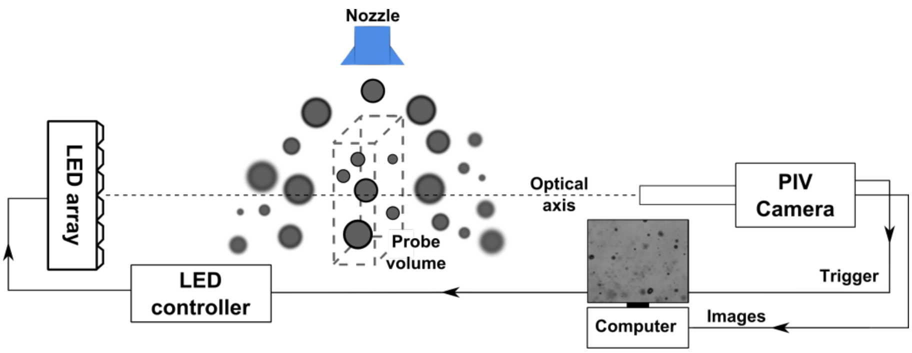

Figure 1. *Shadowgraphy set-up used for the image acquisitions.*

Image processing

The key steps of the image processing are presented on the Figure 2. Starting from the raw image acquired (1); spatial illumination heterogeneity is corrected by subtracting a composite background from each image. The composite background is computed by applying a rank filter on a set of images recorded during the sequence (2).
The droplet shadows present a variable grey level depending on the droplet size, degree of focus and local illumination, there is no unique threshold adapted for an accurate segmentation of all droplets. Therefore, each drop is analyzed individually in order to take into account local image context. The first localization of the drops is achieved by computing the light intensity gradient on whole image. Image areas presenting a gradient higher than the threshold are isolated in sub-images for the subsequent individual sizing (3).
Segmentation of sub-images is realized by the Canny edge detector (Canny, 1986). This method finds object edges from the local gradient maxima. It provides a 1 pixel thin continuous response corresponding to highest values of local gradient. Making the hypothesis that this response corresponds to drop shadow boundaries, drop size is retrieved from the inner area defined by the edge (4).
Finally, the out of focus droplets are rejected because of the low accuracy on their measurements. This rejection is based on the light intensity gradient of the droplet boundary. Sharper is the droplet, stronger is this gradient and vice versa (5).
The droplet tracking aims to pair droplets between the first and the second frame. Two criteria are used. Firstly the droplet diameter should not vary more than 5%. Secondly the droplet displacement is limited to a circular sector oriented along the mean flow direction. The circular sector radius is equal to the maximum speed multiply by the time between the two frames and its opening angle θ is defined as the maximum angle between the main flow direction and the droplet displacement which depend on the turbulence intensity and the nozzle opening angle.
More details about the image analysis method have been presented in a previous paper (De Cock et al., 2014).

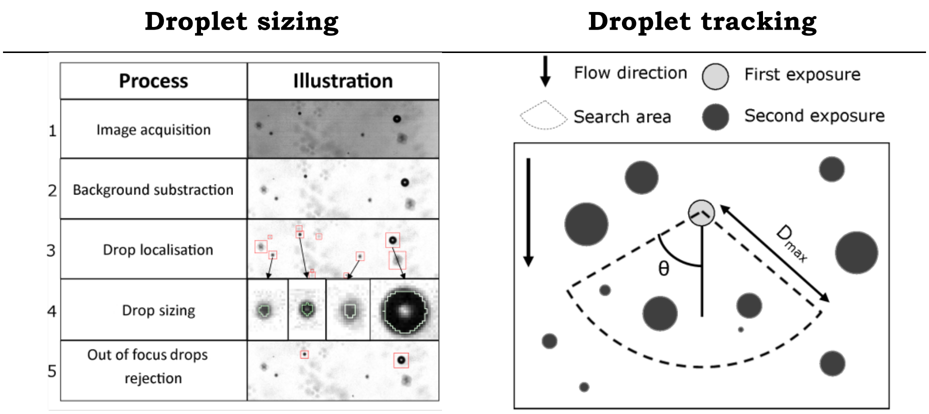

Figure 2. *Flow chart presenting the main steps of the drop sizing algorithm (left). Drop tracking principle using a search area based on a priori knowledge of the flow direction in order to retrieve the same drop on two successive frames (right) (figure adapted from De Cock et al., 2014).*

Spray characterization

The measurements are realized 50cm below the nozzle and cover ¼ of the whole spray assuming the spray symmetry (Figure 3). The scan of the spray is realized by recordings 1500 pair of images per line on 8 lines of 850mm spaced by 10mm. During the recording of the images, the nozzle is moving at 0.0425 m/s along the spray major axis. Finally, the droplet size distribution is retrieved by gathering the data from each scanning line. According to the spray quality, 15 000 to 95 000 droplets were recorded at the end of the whole scan.

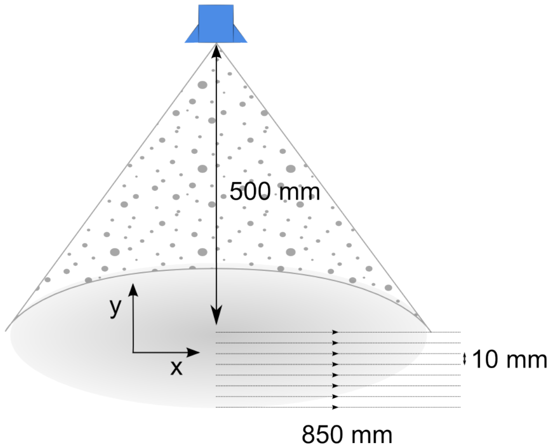

Figure 3. *Scanning pattern used for the characterization of the sprays.*

The six nozzles/pressures combinations corresponding to the 6 spray quality boundaries defined by the ISO draft standard (ISO 25358) are presented below in the Table 1. Tap water was used as liquid and the pressure was set with a maximum relative error of 3%.

Table 1. *Combination of nozzle and pressure defining the different spray class boundaries.*

Spray class boundary	Nozzle	Pressure [Bar]
VF / F	Teejet TP 110 01	4.5
F / M	Teejet TP 110 03	3.0
M / C	Teejet TP 110 06	2.5
C / VC	Teejet TP 80 08	2.5
VC / XC	Teejet TP 65 10	1.5
XC / UC	Teejet TP 65 15	1.5

RESULTS AND DISCUSSION

Drop size distribution

The Figure 4 presents the comparison of the cumulative droplet size distribution for the 6 spray class boundaries. The 6 sprays drop size distributions are well differentiated showing that the shadowgraphy technique is able to measure small and coarse droplets with the same set-up. The smallest droplet had a diameter of 40µm and the largest droplet had a diameter of 1300µm. The coarser sprays present less smooth curves because lower number of droplets recorded.

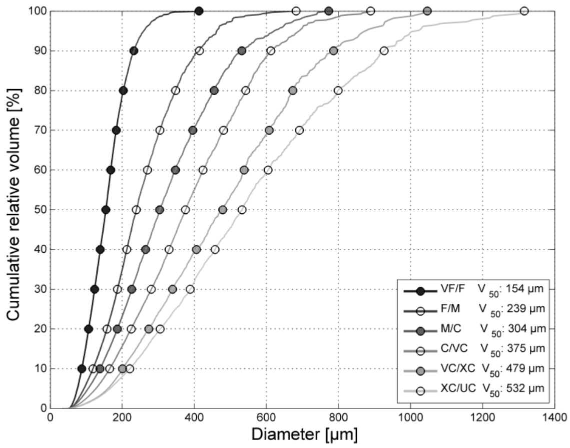

Figure 4. *Cumulative droplet size distribution for the 6 spray class boundaries*

The droplet count, relative span factor, D_{v10}, D_{v50} and D_{v90} are presented below in the Table 2. The relative span factor (RSF) is computed as $(D_{v90}$-$D_{v10})/D_{v50}$. Most of the sprays present an equivalent RSF ranging between 1.2 and 1.3 excepted the finest spray which presents a RFS lower than 1. This value may be under estimated because the technique is rejecting all the smaller droplets (> 40µm) which can significantly increase the value of D_{v10} and then decrease the RSF.

Table 2. *Main parameters measured for each spray class boundaries.*

Spray class boundaries	Dv10 [µm]	Dv50 [µm]	Dv90 [µm]	Relative span factor	Droplet count
VF / F	88	154	232	0.94	95 398
F / M	119	239	414	1.24	46 756
M / C	138	304	532	1.30	39 947
C / VC	165	375	612	1.19	28 817
VC / XC	201	479	786	1.22	15 552
XC / UC	221	532	927	1.33	20 084

Spatial distribution of the droplet densities

The Figure 5 presents the droplet density at different distance from the jet center on the y axis as draw on the Figure 3. The relative droplet density is defined as the droplet count at this distance divided by the overall number of droplet counted. The droplet density is linearly decreasing whilst the distance increase from the jet center. For all the sprays, the droplet density is quite low (<5%) at 7cm from the jet center. It may be relevant to extend the scanning area by adding some scanning lines in order to be sure to catch the whole spray. However, the further scanning lines have a little weight on the overall spray characteristics because of their low relative spray volume content by comparison with the first scanning lines.

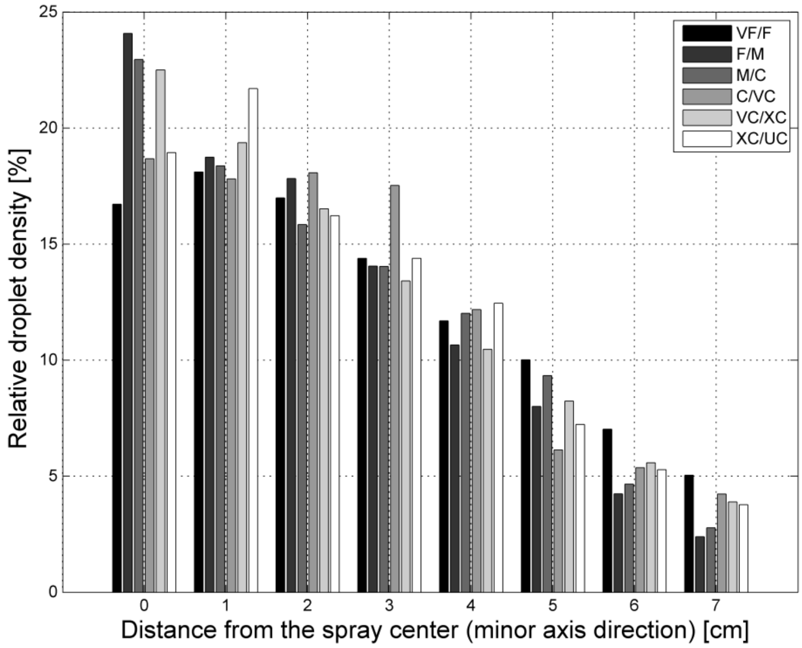

Figure 5. *Relative droplet density in respect with the distance from the jet center for the 6 spray class boundaries.*

Spatial distribution of the droplet densities

The Figure 6 presents the droplet spatial repartition of the density for each nozzle. The point (0,0) corresponding to the spray center. The highest density corresponding to the white tone is often encountered at the spray center. For the VF/F nozzle there is a shift of the highest droplet density may be induced by the nozzle displacement that could affect more the smaller droplets. The spray shapes are directly affected by the nozzle opening angle showing a much wider spray for the 110° nozzles than for the 65° nozzles.

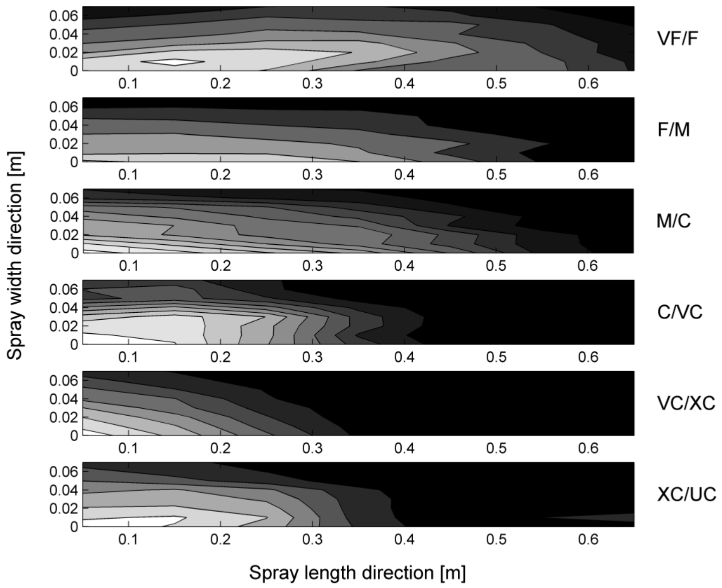

Figure 6. *Relative droplet density maps for each spray. The clear and the dark tones correspond to the higher and the lower droplet densities respectively.*

CONCLUSION

A shadowgraphy method was tested on the 6 spray class boundaries which are defined in the ISO draft standard (ISO 25358). The technique showed a good capability to correctly distinguish the 6 different sprays using the same set-up configuration. These results show that shadowgraphy can be a real alternative to the laser based technique for the characterization of agricultural spray. More work has to be done on the optimization for the agricultural sprays of the main parameters (magnification factor, time lapse between two frames, algorithm parameters …). Indeed the lower threshold of the droplet size may be a problem for the finer sprays. The scanning strategy should also be improved in order to reduce the error due to the spray under sampling.

ACKNOWLEDGEMENT

I would like to thanks the FNRS for the funding of my PhD through the F.R.I.A. PhD grant.

REFERENCES

Canny J. 1986. A computational approach to edge detection. *IEEE Transactions on Pattern Analysis and Machine Intelligence* 8:679–698.

Cousin J, Berlemont A, Ménard T, Grout, S. 2012. Primary breakup simulation of a liquid jet discharged by a low-pressure compound nozzle. *Computers and Fluids* 63:165–173.

De Cock N, Massinon M, Lebeau F. 2014. Agricultural spray measurement by high-speed shadow imagery. *Aspects of Applied Biology* **122,** *International Advances in Pesticide Application*, pp. 363-369.

Massinon M, Boukhalfa H, Lebeau F. 2014. The effect of surface orientation on spray retention. *Precision agriculture*, *15*:241-254.

Massinon M, Lebeau F. 2012. Experimental method for the assessment of agricultural spray retention based on high-speed imaging of drop impact on a synthetic superhydrophobic surface. *Biosystems Engineering* 112:56–64.

Matthews G, Bateman R, Miller P. 2008. Pesticide application methods, Third Edition. John Wiley & Sons